Supplemental Materials

Molecular Biology of the Cell

Marchenko et al.

Supplemental Materials

List of Supplemental Materials

1. Supplemental methods. Description of FiloTracker Software

We developed an algorithm, implemented in Matlab, for tracking dendritic filopodial dynamics. The algorithm, which we call FiloTracker, can analyze a binary stack derived from DIC, phase contrast or fluorescence movies by automatically skeletonizing the filopodia into connected linear segments.

To produce a binary image for the algorithm two feature extraction steps were performed: edge-detection and foreground-background segmentation. At that point all the images in the stack are binary and ready for skeletonizing and tracking. FiloTracker then implements the annealed particle filtering algorithm originally developed to analyze articulated body motion in the computer vision field (Isard and Blake, 1998); the main idea is to compute the best configuration (the set of parameters that describes the object shape) as a statistical average over an ensemble of possible configurations, rather than searching for the best parameter set through some minimization procedure. Each filopodium in our method is represented by its skeleton, which is a non-self-intersecting polygonal chain with a fixed number, n, of segments of equal lengths. The skeleton is parametrized using the angles between the segments and the length of the segments. The default value of n is 4, but it may be adjusted by the user to achieve better results for extremely curvy filopodia. To initiate the skeletonization process, the user chooses filopodia in the first image of the stack by clicking pixel pairs at the base and tip of each filopodium. For each consecutive image, the algorithm first generates a sufficiently large random set of possible configurations in the vicinity of the skeleton from the previous frame; the only required

constraint is that the base of all configurations is fixed. We then use pixel values from the new image to compute weights for these configurations, where weight is a measure of how closely a configuration lines up with the pixels in the new frame. Finally, in the new frame, the algorithm computes the configuration for the new skeleton as a weighted vector sum of all configurations from the original set. Full details on the mathematics behind the algorithm can be found in (Isard and Blake, 1998). Once the best fit filopodium is found on each consecutive frame, the length measurements are recorded into the output file. We found that image acquisition at 1 frame per second was sufficiently fast for highly precise tracking.

We validated our model with two independent test procedures. For the first, we generated a spatial simulation of a model filopodium that randomly grows, retracts and flails. The filopodium was simulated as a non-self-intersecting polygonal chain with a given bending modulus and given polymerization /depolymerization rates. Random force was applied at each node of the chain to generate realistic filopodia dynamics. Then, we used FiloTracker to measure the filopodium length. We compared the exact length values to lengths from the FiloTracker output and evaluated algorithm's performance *(FigureS5).* In the second validation we tracked filopodia by hand and compared hand-tracked filopodia length measurements to FiloTracker output *(FigureS6).*

2. Supplemental Tables and Figures

Table S1. Parameter values for nominal case result in ARF and myosin localization profiles that match experimental data.

Forces/Processes	Parameter	Physical significance	Value range	Units	Reference/source
Force due to viscous flow of actin	η	Viscosity	100	$pN \cdot s$	(Bausch *et al.*, 1998)
Myosin contractility	σ_0	myosin contractility	25	$\frac{pN \cdot \mu m}{molecule}$	Non-dimensional analysis
Adhesion Force	ζ	drag force coefficient	100	$\frac{pN \cdot s}{\mu m^2}$	(Chan and Odde, 2008)
Myosin binding	k_{off} / $k_{on,\ Kd}$	myosin binding rate	0.9310	nM	(Norstrom *et al.*, 2010)
Actin polymerization	v_p	polymerization rate	0.9	$\frac{\mu m}{s}$	(Tatavarty *et al.*, 2012)
Initial filopodia length	L_0	initial length	1	µm	experimental data
Diffusion	D	diffusion coefficient	0.04	$\mu m^2/s$	Calculated from myosin random walk
Resistive force	β	Resistive force coefficient	5250	$\frac{pN \cdot s}{\mu m^{\blacksquare}}$	Parameter screening
Unbound myosin concentration	m_0	Unbound myosin	25	Molecules/µm	Non-dimensional analysis
Membrane tension	Tκ	Tension force on the cell membrane due to curvature	2.0	pN	(Hochmuth, 1996)

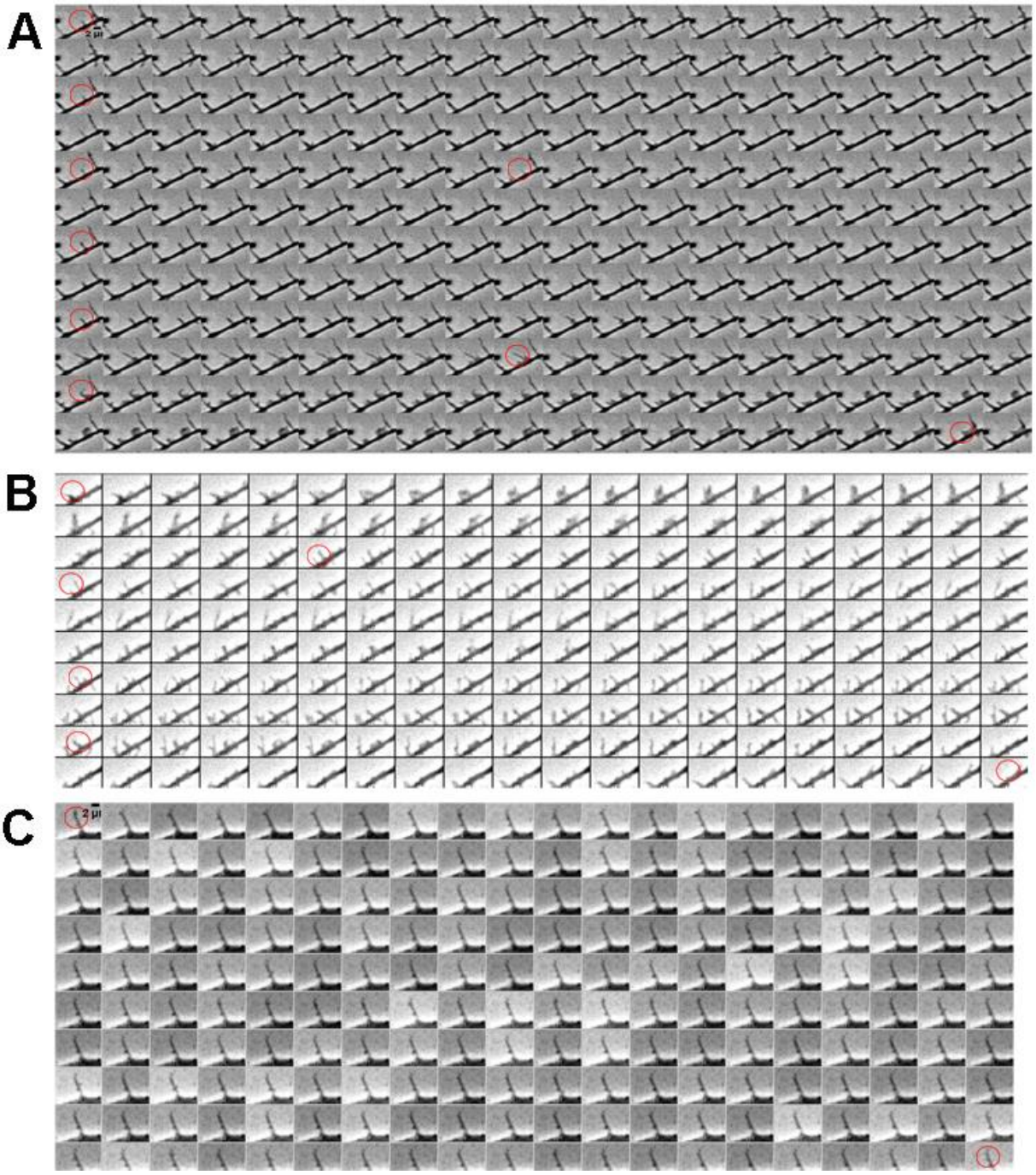

Figure S1. Montage of sequential phase-contrast images taken with acquisition rate 1f/s of different types of filopodial motility A. Continuously motile filopodia exhibit regular lengths fluctuations and have long lifetimes. B. Transiently motile filopodia have short lifetimes with burst dynamics. C. Non-motile filopodia have constant lengths over long periods of times.

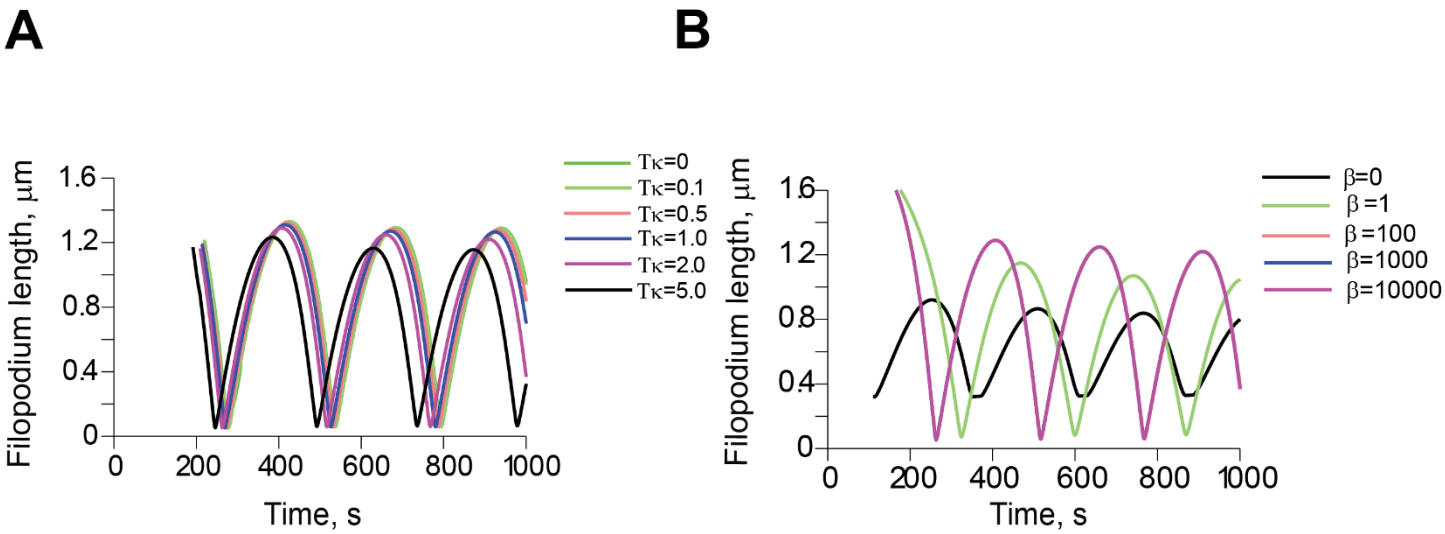

Figure S2. Sensitivity analysis for parameters Tκ. and β. A. Model's output for a Tκ range [0,5.0]$\boldsymbol{pN}$. B. β values ≥100 result in steady-state with oscillations all lying on the same curves . Parameters used for the simulations are L_0 =1, k_{off}=0.13, k_{on}=0.12,v_p=0.9, m_0 = 25, η =100, ζ=100, σ_0 =25, D=0.04

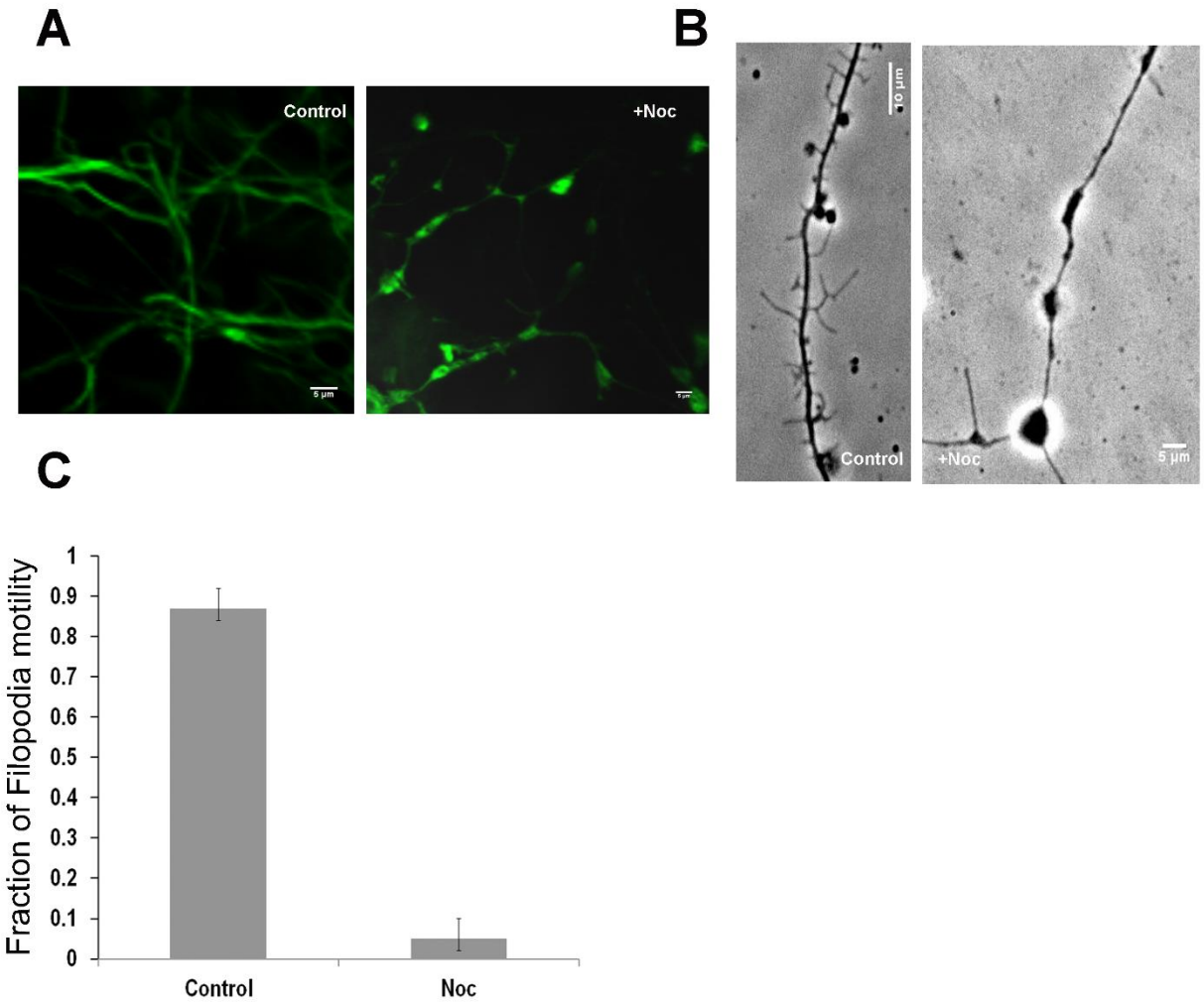

Figure S3. Nocodazole treatment reduces filopodia motility and number. Control neuron cultures and neurons treated with 1.6µM nocodazole after 1hr incubation at 37°C on DIV4 shown with (A) 488-Alexa tubulin staining or (B) phase-contrast microscopy. C. fraction of motile filopodia in nocodazole treated cells, t-test, $P<0.05$ (32 filopodia, 8 neurons).

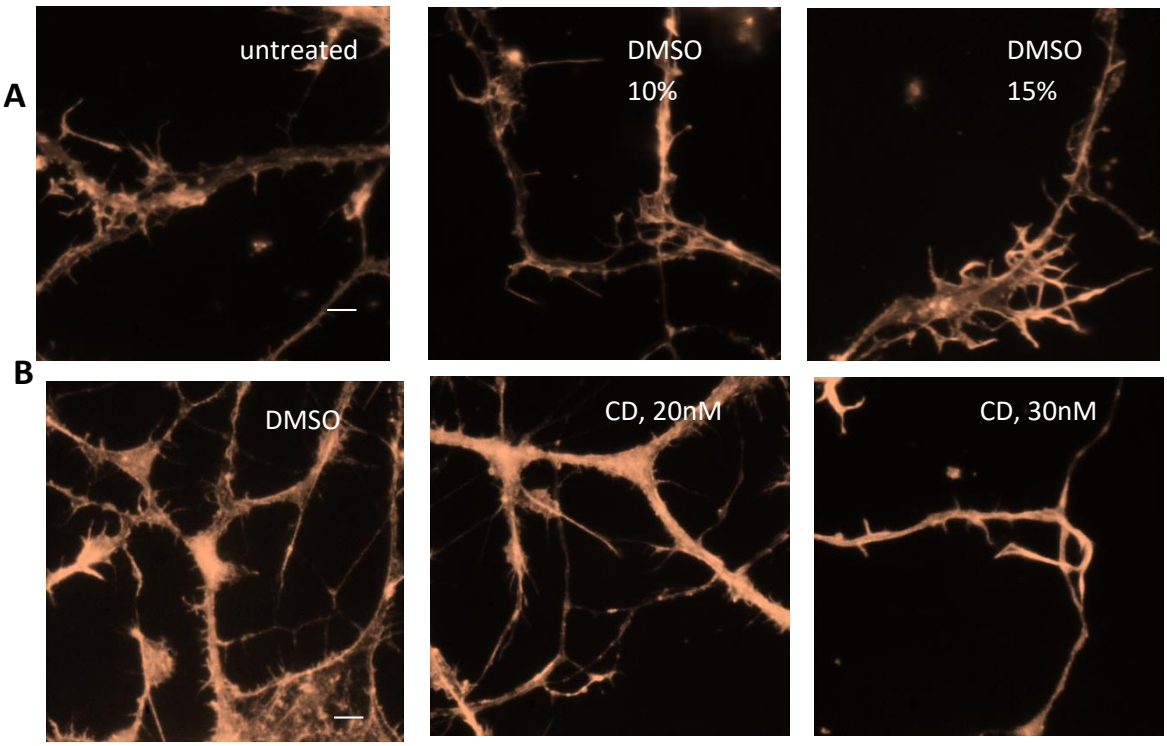

Figure S4. Cytochalasin D and DMSO treatments have not disrupted filamentous actin in aconcentrations used in the drug assays as shown by rhodamine staining of F-actin following drug administration. A. Control DMSO treatment did not have significant effect on density and structure of filamentous actin. B. Cytochalasin D treatment at treatment did not have significant effect on density and structure of filamentous actin at 20nM. Treatment with 30nM CD resulted in significant reduction of filopodia motility and changes in actin network compared to control. Scale bar 10μm

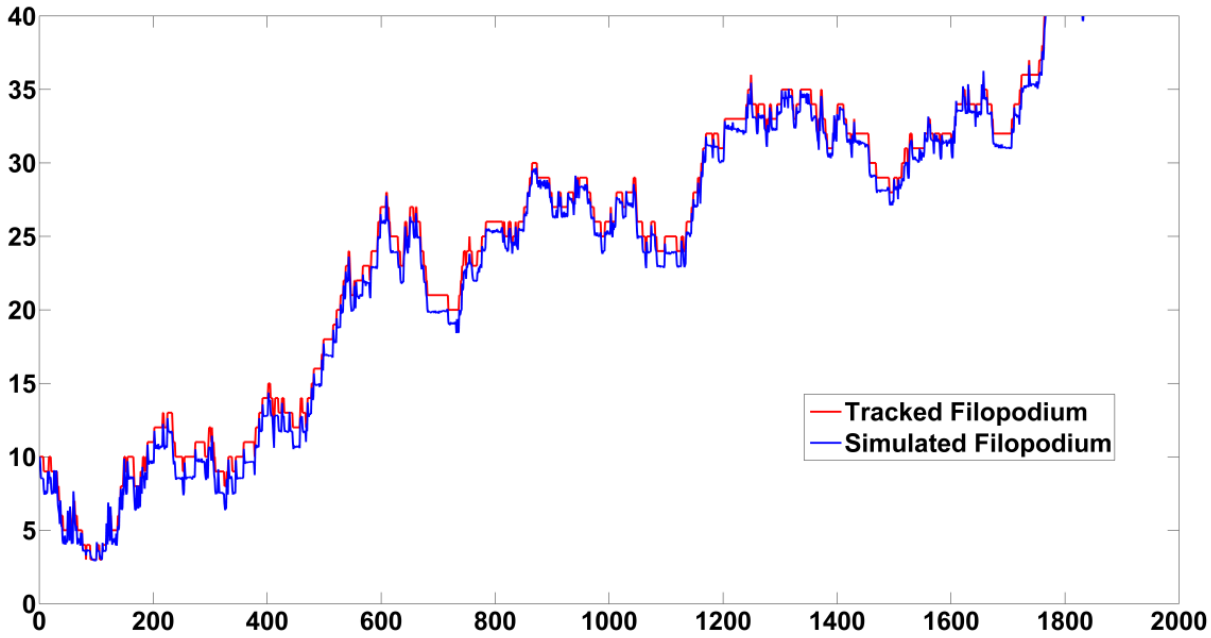

Figure S5. Filo tracker algorithm (red line) length measurements closely follow computer-generated binary image of filopodium dynamics simulation (blue line) with standard error E=0.88%.

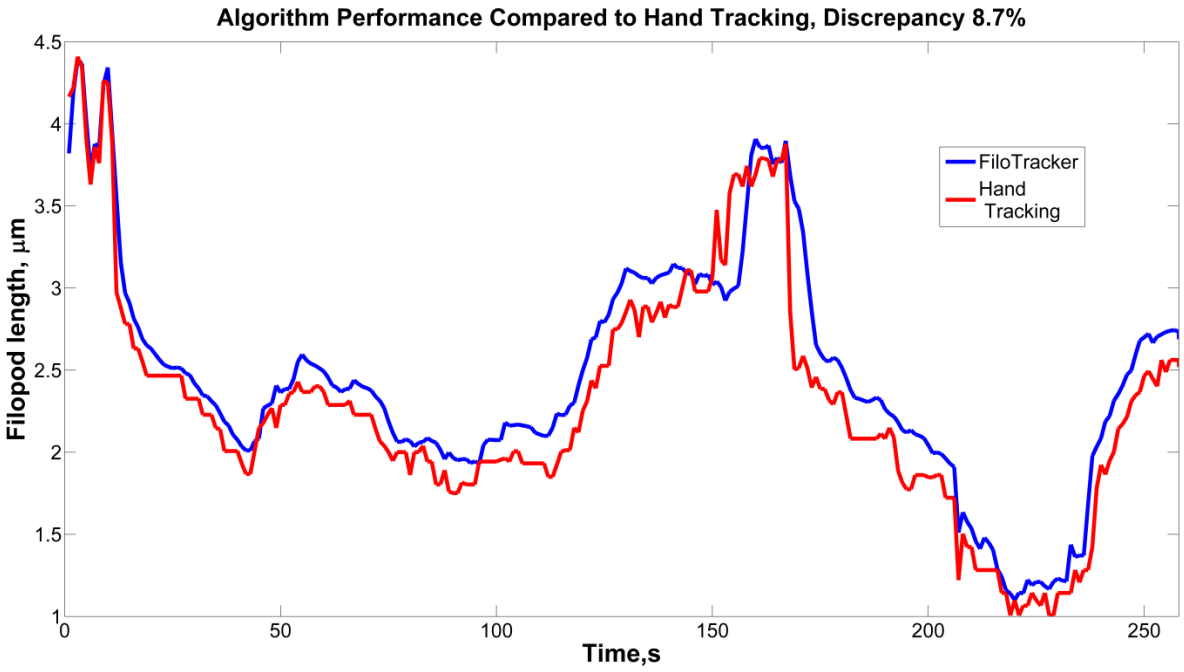

Figure S6. FiloTracker algorithm (blue line) length measurements output matches hand tracked filopodium lengths from live phase-contrast microscopy recording (blue line) with standard error E = 8.7%.

3. Legends to Supplemental Movies

MovieS1. Filopodium length tracked with FiloTracker Software (red dotted line), acquisition rate =4f/s, play rate 100 f/s, rat hippocampal neuron culture, DIV4, poly-L-lysine 0.5mg/ml, bar 10µm

MovieS2A. - Filopodia motility after 20nM cytochalasin D treatment. rat hippocampal neuron culture, DIV4-7, poly-L-lysine 0.5mg/ml, acquisition rate =1f/s, play rate 100 fr/s ,bar 10µm,

MovieS2B .Filopodia motility after 10nM cytochalasin D treatment, rat hippocampal neuron culture, DIV4-7, poly-L-lysine 0.5mg/ml, acquisition rate =1f/s, bar 10µm, play rate 100 fr/s

MovieS3A. Filopodia motility on poly-L-lysine substrate with 0.05mg/ml, rat hippocampal neuron culture, DIV4-7, acquisition rate =1f/s, bar 10µm, play rate 100 fr/s

MovieS3B. Reduced filopodia motility on poly-L-lysine substrate with 0.01mg/ml, rat hippocampal neuron culture, DIV4-7, acquisition rate =1f/s, play rate 100 fr/s, bar 5µm

MovieS3C. Reduced filopodia motility on poly-L-lysine substrate with 1.00mg/ml, rat hippocampal neuron culture, DIV4-7, acquisition rate =1f/s, play rate 100 fr/s, bar 10µm

MovieS4. Increased filopodia motility and length in the presence of 2.5µM blebbistatin, rat hippocampal neuron culture, DIV4-7, acquisition rate =1f/s, play rate 100 fr/s, bar 10µm

4. Supplemental References

1. Isard M, Blake A. 1998. Conditional density propagation for visual tracking. *International Journal of Computer Vision* 29: 4
2. Norstrom MF, Smithback PA, Rock RS. 2010. Unconventional processive mechanics of non-muscle myosin IIB. *J Biol Chem* 285: 26326